

S-Oxygenation of Thiocarbamides. 3. Nonlinear Kinetics in the Oxidation of Trimethylthiourea by Acidic Bromate[†]

Tabitha R. Chigwada,[‡] Edward Chikwana,[§] Tinashe Ruwona,^{||} Olufunke Olagunju,^{||} and Reuben H. Simoyi^{*||}

Department of Chemistry, Portland State University, Portland, Oregon 97207-0751, C. Eugene Bennett

Department of Chemistry, West Virginia University, Morgantown, West Virginia 26506-6045, and Department

of Chemistry, California State University—Chico, Chico, California 95929-0210

Received: June 22, 2007; In Final Form: August 8, 2007

The oxidation of trimethylthiourea (TMTU) by acidic bromate has been studied. The reaction mimics the dynamics observed in the oxidation of unsubstituted thiourea by bromate with an induction period before formation of bromine. The stoichiometry of the reaction was determined to be 4:3, thus $4\text{BrO}_3^- + 3\text{R}_1\text{R}_2\text{C}=\text{S} + 3\text{H}_2\text{O} \rightarrow 4\text{Br}^- + 3\text{R}_1\text{R}_2\text{C}=\text{O} + 3\text{SO}_4^{2-} + 6\text{H}^+$. This substituted thiourea is oxidized at a much faster rate than the unsubstituted thiourea. The oxidation mechanism of TMTU involves initial oxidations through sulfenic and sulfinic acids. At the sulfinic acid stage, the major oxidation pathway is through the cleavage of the C–S bond to form a reducing sulfur leaving group, which is easily oxidized to sulfate. The minor pathway through the sulfonic acid produces a very stable intermediate that is oxidized only very slowly to urea and sulfate. The direct reaction of aqueous bromine with TMTU was faster than reactions that form bromine, with a bimolecular rate constant of $(1.50 \pm 0.04) \times 10^2 \text{ M}^{-1} \text{ s}^{-1}$. This rapid reaction ensured that no oligooscillatory bromine formation was observed. The oxidation of TMTU was modeled by a simple reaction scheme containing 20 reactions.

Introduction

We recently embarked on a series of studies aimed at elucidating the kinetics and mechanisms of the oxidation of thio compounds by oxyhalogen ions.² The primary aim of this series of experiments is to elucidate the mechanisms for the recently discovered chemical oscillatory systems that involve oxyhalogen–sulfur chemistry.^{3–6} The use of small-molecule organosulfur compounds discouraged the sulfur atom's propensity to polymerize, limiting degree of aggregation to only as far as the dimeric species. This greatly improved our control and reproducibility of our kinetics results.

Our initial motivation in studying the interactions of oxyhalogens and organosulfur compounds was the discovery of a special subset of two-component oscillators that involved primarily the oxidation of a sulfur center in a continuously stirred tank reactor, CSTR.⁷ In fact, the number of chemical oscillators that involve oxyhalogens and sulfur compounds, on their own, far outstrip the rest of the other known oscillators. Remarkably, the range and wealth of exotic dynamics observed in this new subset rivals and even surpasses the more well-known venerable Belousov–Zhabotinskii oscillating system.⁸ Among some of the features displayed by these systems are stochastic triggering, clock behavior, stirring rate effects, homoclinic chaos,⁹ and even symmetry-breaking bifurcations fueled by convective instabilities.¹⁰ A comprehensive and full description of such features is possible only if the kinetics and mechanisms of the relevant reactions are known in detail. For example, a characterization

of the bromate–thiocyanate oscillator was not possible until the mechanism of oxidation of the thiocyanate ion by acidic bromate was elucidated.¹¹

Thiourea is the simplest and smallest thiocarbamide that contains the thiouredo group.¹² Despite its simplicity, its oxidation by iodate,¹³ chlorite,¹⁴ and bromate¹⁵ have all been found to give complex kinetics behavior. Iodate oxidations give oligooscillatory dynamics,¹³ bromate oxidations give clock and oscillatory dynamics⁷ and those with chlorite have shown chaotic dynamics^{9,16} and spatiotemporal patterns.¹⁷ While the chemistry of oxyhalogens has been exhaustively studied,^{18,19} not as much is known about organosulfur chemistry. The well-known chemistry of oxyhalogens was insufficient to explain all observed nonlinear dynamics.

Thiourea and its derivatives are a group of very active biological molecules.^{20–26} The major pathway to their bioactivation is oxidative and specifically via S-oxygenation in which there is a successive addition of oxygen to the sulfur center until oxidative saturation is attained at sulfate.^{25,27} Thioureas are oxygenated by flavin-containing monooxygenases²⁵ to form reactive sulfenic acids that reversibly react with glutathione to drive oxidative stress through a redox cycle.

Our second motivation in studying oxidation mechanisms of thiocarbamides is the varied metabolic effects they induce based on very small changes in substituents. In order to rationally design thiourea-containing drugs, it is necessary to develop structure–toxicity relationships. For example, a series of closely related compounds, *N*-(*p*-bromophenyl)-, *N'*-(4-imidazolylethyl)-, *N*-(*p*-chlorophenyl)-, and *N*-(*p*-methoxyphenyl)thioureas, all gave vastly varying degrees of toxicities^{28,29} as evidenced by LDH leakage, but no additional information is available regarding a possible mechanism for cytotoxicity that could explain these observations. However, in all cases, the formation

[†] This is the third in a series of five papers on the S-oxygenation of substituted thiocarbamides. See ref 1.

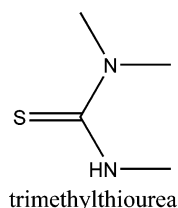
[‡] West Virginia University.

[§] California State University—Chico.

^{||} Portland State University.

of the sulfenic acid during bioactivation was essential. A series of simple thiocarbamide compounds that can easily be studied is thiourea, dimethylthiourea, trimethylthiourea, and tetramethylthiourea. Dimethylthiourea is a small molecule that efficiently scavenges toxic oxygen metabolites in vitro and reduces oxidative injury in many biological systems.^{30–32} It is the most efficient scavenger for hydrogen peroxide, hydroxyl radical, and hypochlorous acid.³³

This paper reports on the oxidation mechanisms of a substituted thiourea, trimethylthiourea, by acidic bromate. While



the biological activities of thiourea and dimethylthiourea are well documented, not much has been reported on these other substituted thiourea compounds. How would their oxidation mechanisms differ? What metabolites are formed in the oxidation pathway, if any? The use of a strong oxidant, much stronger than the standard biological oxidants in the form of hydrogen peroxide and superoxide, can enable the oxidation of the thioredo group all the way to the urea analogue. Previous studies from our laboratory had shown that the bromate–thiourea reaction is a very reproducible oscillatory clock reaction that generates oscillatory behavior in a flow reactor.⁷

Experimental Section

Materials. The following reagents were used without further purification: trimethylthiourea (TCI), sodium bromate, perchloric acid (70–72%), sodium bromide, bromine, sodium perchlorate, sodium thiosulfate (Fisher). All the major reactants were assumed to be of high enough purity so there was no need for standardization. Bromine solutions, being volatile, were kept capped and were standardized before each set of experiments.

Methods. Experiments were carried out at 25 ± 0.5 °C. The ionic strength was maintained at 1.0 M (NaClO_4) in all experiments. Most of the reactions were performed on a Hittech Scientific SF-61DX2 double-mixing stopped-flow spectrophotometer with an F/4 Czerny–Turner MG-60 monochromator and a spectra scan control unit. The signal from the spectrophotometer was amplified and digitized via an Omega Engineering DAS-50/1 16-bit A/D board interfaced to a computer for storage and data analysis. Reaction progress was followed by monitoring the production of Br_2 at 390 nm, where it has an absorption peak. The direct reactions between bromine and TMTU were monitored by following the consumption of bromine at 390 nm on the stopped-flow spectrophotometer. Some reactions were studied by observing the TMTU peak at 216 nm. Figure 1 shows the superimposition of the three spectra for TMTU, trimethylurea (TMU), and aqueous bromine. The bromine peak was isolated from the organic species, and thus formation of bromine could be followed without any interference. The reaction could be followed at 216 nm only in the very initial stages before accumulation of products that absorb much more strongly at this wavelength. For the observation of longer time scales, the contribution from other species could be subtracted off through an extrapolation technique (see Figure 7).

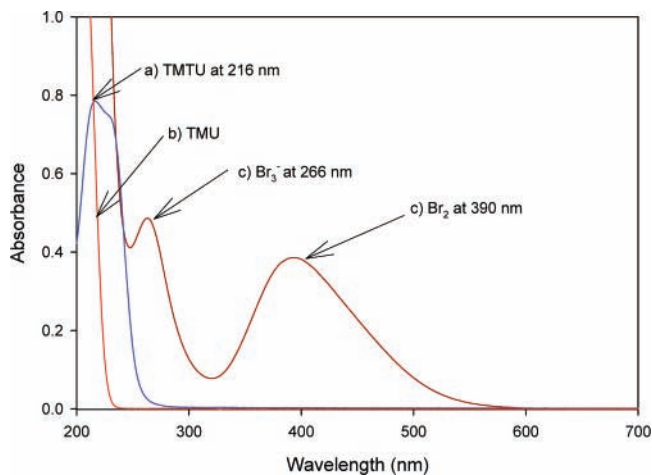


Figure 1. Spectral scans of TMTU, TMU, and bromine. TMTU absorbs in the UV region at 216 nm; TMU has no significant absorbance in either the near-UV or vis regions; bromine solutions absorb at two wavelengths, 266 and 390 nm. The 390 nm peak is isolated and can be used to quantify bromine concentrations.

Stoichiometric Determinations. Stoichiometric determinations were performed by the use of several complementary techniques: titrimetric, gravimetric, and spectrophotometric. By varying the amounts of bromate while keeping the reducing substrate concentration low and constant (in highly acidic conditions to speed up the reaction), we could determine the required stoichiometry at the point just before the reaction solution produced bromine. Excess bromate was acidified and mixed with excess iodide, and the liberated iodine was titrated against standard sodium thiosulfate with freshly prepared starch as indicator. Bromine was evaluated from its absorbance at 390 nm (absorptivity coefficient $142 \text{ M}^{-1} \text{ cm}^{-1}$) as well as from an iodometric technique.

Tests for Adventitious Metal Ion Catalysis. Water used for preparing reagent solutions was obtained from a Barnstead Sybron Corporation water purification unit capable of producing both distilled and deionized water (Nanopure). Not much difference was observed in the general reaction kinetics observed with distilled and deionized water. We utilized inductively coupled plasma mass spectrometry (ICPMS) to quantitatively evaluate the concentrations of a number of metal ions in the water used for our reaction medium. ICPMS analysis showed negligible concentrations of iron, copper, and silver and approximately 1.5 ppb cadmium and 0.43 ppb lead as the most abundant metal ions.

Results

Stoichiometry. Reactions were run in excess oxidant, and after a reasonable incubation period, the excess oxidizing power was subsequently determined by iodometric techniques. By varying initial bromate concentrations, the titer obtained from an iodometric technique could be related to the excess oxidizing power left after consumption of the TMTU. A plot of this titer volume versus initial bromate concentration was linear (see Figure 2). Extrapolating this linear plot to the bromate concentration axis gives the exact amount of bromate needed to completely consume the substrate with nothing left to participate in the iodometric titration. This stoichiometry is shown in reaction R1. Experimental data in Figure 2 had a fixed concentration of 0.0025 M TMTU. The intercept value for this series of titrations is $48.79/14\,280$, which gives a stoichiometric bromate concentration of $0.003\,42 \pm 0.000\,13$

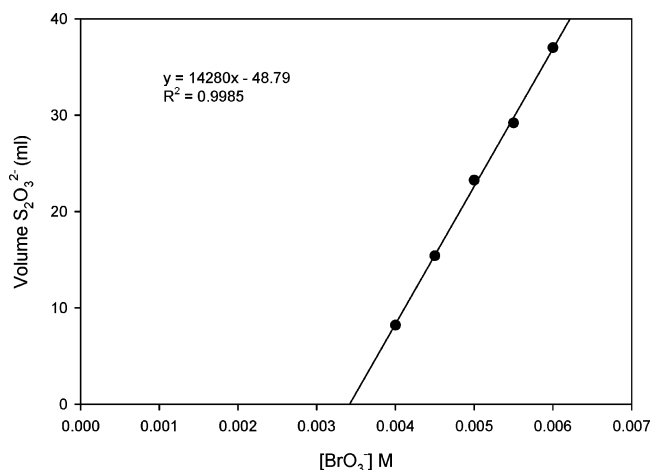
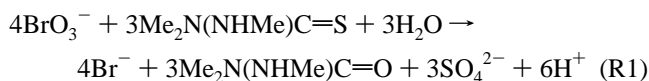
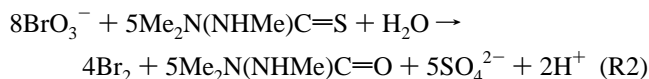


Figure 2. Titrimetric stoichiometric determination for the bromate–TMTU reaction. The excess oxidant is quantitatively transformed into iodine equivalents through addition of excess KI. Thiosulfate titer volume is plotted against the initial bromate concentration. The intercept on the bromate axis denotes the bromate concentration needed to just oxidize TMTU with none left to produce iodine. In this plot, a constant 0.0025 M TMTU needed 0.003 42 M bromate; which translates to the 4:3 ratio shown in reaction 1.

M. This gives the 4:3 stoichiometric ratio shown in reaction R1:



The reaction produced aqueous bromine as a final product when the oxidant to reductant ratio, $R = [\text{BrO}_3^-]_0/[\text{Me}_2\text{NN}(\text{HMe})\text{C}=\text{S}]_0$, exceeded 4:3. With a high excess of bromate, the bromate:TMTU ratio was observed to be strictly 8:5:



Under these conditions of high excess of bromate over TMTU, the amount of bromine obtained was determined by the amount of substrate used, and thus the spectrophotometric determination at 390 nm was used as a complementary technique to evaluate the stoichiometry of reaction R2. This linear relationship is valid between ratios 4:3 and 8:5. At ratios greater than 8:5, the amount of bromine formed became invariant. The maximum bromine absorbance obtained in Figure 4, for example, confirms the stoichiometry of reaction R2. Another more accurate method of evaluating the stoichiometry of reaction R1 was to use varying amounts of excess bromate and evaluate the time taken for bromine formation (see Figure 4). Solutions with lower than 4:3 stoichiometry will have no induction period, or rather, will have infinitely long induction periods. The inverse of the induction period under these conditions is zero. A plot of the inverse of the induction period versus bromate concentrations is linear (plot not shown), with the intercept at exactly the stoichiometry of reaction R1. Several gravimetric analysis experiments were performed in which sulfate was determined as a barium sulfate precipitate. Excess bromate conditions precipitated barium bromate, which delivered anomalously high precipitate yields. The excess bromate, in such cases, was first neutralized with excess iodide to form bromine, thus precluding precipitation of barium bromate (see last three runs in Table 1). Table 1 shows the data which confirm that, within experimental error, all the sulfur on TMTU ended up as sulfate

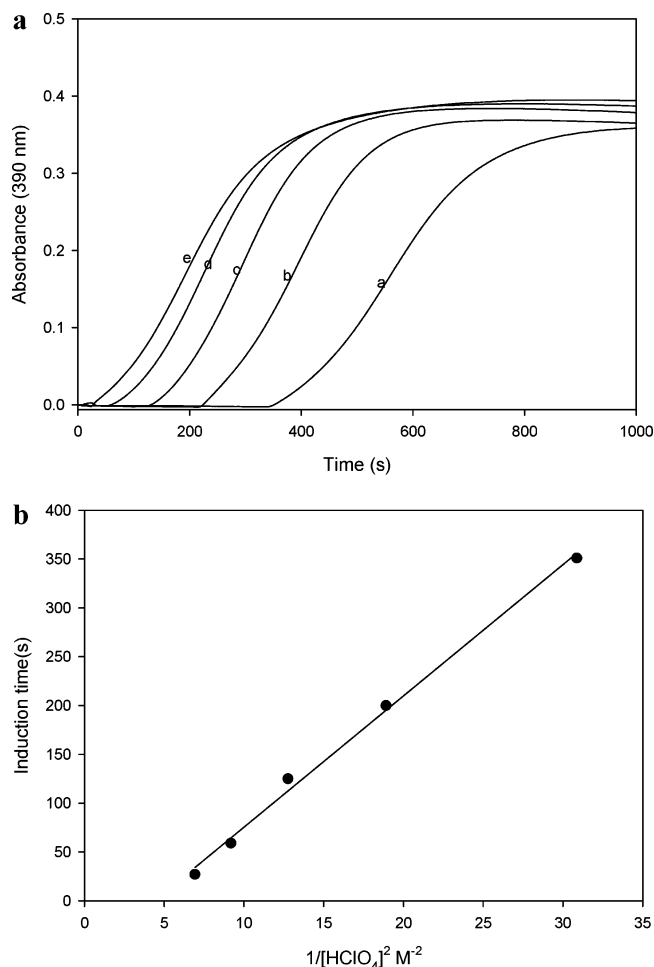


Figure 3. (A) Effect of acid on the BrO_3^- –TMTU reaction in excess bromate. Acid markedly decreases the induction period before formation of bromine. There is an abrupt, sudden, and autocatalytic formation of bromine. Acid also catalyzes the rate of formation of bromine at the end of the induction period. Fixed concentrations: $[\text{TMTU}]_0 = 3.5 \times 10^{-3}$ M, $[\text{BrO}_3^-]_0 = 3.0 \times 10^{-2}$ M. Variable concentration: $[\text{HClO}_4]_0 =$ (a) 1.8×10^{-1} M, (b) 2.3×10^{-1} M, (c) 2.8×10^{-1} M, (d) 3.3×10^{-1} M, or (e) 3.8×10^{-1} M. (B) Response of the induction period to acid for the data shown in panel A. The inverse square dependence on acid indicates that processes that are prerequisites for the formation of bromine depend on acid to the second power. A shorter induction period denotes a faster reaction.

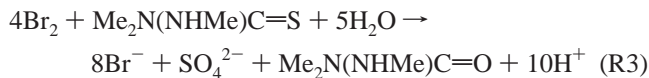
TABLE 1: Gravimetric Determination of BaSO_4 from the BrO_3^- /TMTU Reaction^a

BrO_3^- (mol)	TMTU (mol)	BaSO_4 (g)	% yield
0.001 33	0.001 00	2.302	98.6
0.001 33	0.001 00	2.224	95.3
0.001 33	0.001 00	2.235	95.7
0.001 33	0.001 00	2.310	99.0
0.001 33	0.001 00	2.214	95.6
0.003 00	0.001 00	2.289	98.1
0.003 00	0.001 00	2.268	97.2
0.003 00	0.001 00	2.285	97.9

^a Mean percentage yield of sulfate was $(97.1 \pm 1.58)\%$.

after oxidation with a $(97.1 \pm 1.58)\%$ yield, based on the expectation that 1.0 mol of TMTU gave 1.0 mol of sulfate. This gravimetric analysis was important since some previous studies into the oxidation of thiourea compounds have isolated at least two stable oxoacid metabolites in acidic environments.^{34–36}

A combination of titrimetric and spectrophotometric techniques established a 4:1 ratio for the direct reaction of bromine with TMTU:



The change (decrease) in pH, based on the stoichiometry of reaction R3, could also be simultaneously monitored during the titration.

Reaction Kinetics. The reaction, when monitored at 390 nm, shows no activity at this wavelength for an initial period whose duration is determined by the initial reagent concentrations. If the cell potential of the reaction mixture is monitored in a batch reaction mode, the same period of quiescence observed at 390 nm is also observed. At the end of this induction period, the cell potential rises rapidly at the same time the absorbance increases gradually. The potential stabilizes at a value of approximately 1.10 V (after the calomel reference offset is considered). The dominant couple in the reaction medium at this point appears to be the $2\text{Br}_2/\text{Br}^-$ couple ($E_0 = 1.08 \text{ V}$).⁷ There is a decrease in the absorbance peak at 216 nm initially, but this quickly saturates since products formed in the reaction also absorb strongly at this wavelength.

Effect of Acid. As with most oxyhalogen-based reactions, acid is a very strong catalyst in this reaction. Higher acid concentrations reduce the induction period and increase the rate of formation of bromine at the end of the induction period (Figure 3A). Acid, in itself, was not a reactant in this reaction and did not influence the maximum amount of bromine formed, only the time taken to attain this maximum. There was a strong square inverse acid concentration dependence of the induction period (Figure 3B). Formation of bromine indicates a particular event in the evolution of the reaction, and a decrease in this induction period indicates faster reaction kinetics. The inverse square acid dependence of the induction period indicates that the rate-determining step for processes that lead to the formation of bromine must be dependent on acid to the second power.

Effect of Bromate. Bromate concentrations also decreased the induction period (see Figure 4), but in contrast to acid dependence, this induction period depended only on the inverse concentration of bromate. The final amount of bromine formed was invariant to changes in bromate concentration as long as

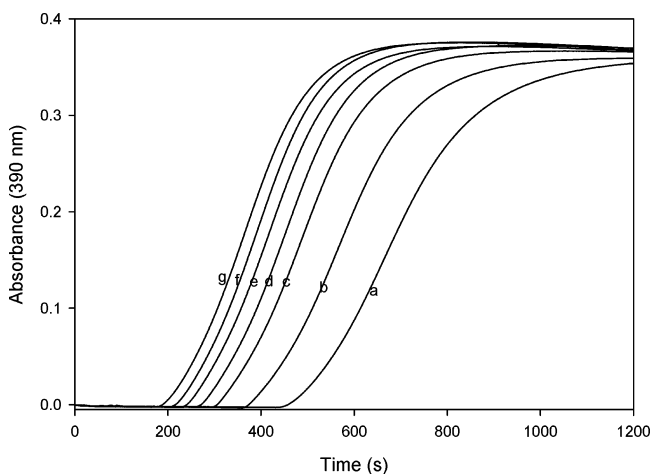


Figure 4. Effect of bromate in conditions where $[\text{BrO}_3^-]_0 \gg [\text{TMTU}]_0$. In this mode, the amount of bromine formed is dependent on the initial TMTU concentrations. Bromate also decreases the induction period but not as dramatically as in the case with acid. Fixed concentrations: $[\text{TMTU}]_0 = 3.4 \times 10^{-3} \text{ M}$, $[\text{HClO}_4]_0 = 2.5 \times 10^{-1} \text{ M}$. Variable concentration: $[\text{BrO}_3^-] =$ (a) $1.5 \times 10^{-2} \text{ M}$, (b) $1.75 \times 10^{-2} \text{ M}$, (c) $2.0 \times 10^{-2} \text{ M}$, (d) $2.25 \times 10^{-2} \text{ M}$, (e) $2.5 \times 10^{-2} \text{ M}$, (f) $2.75 \times 10^{-2} \text{ M}$, or (g) $3.0 \times 10^{-2} \text{ M}$.

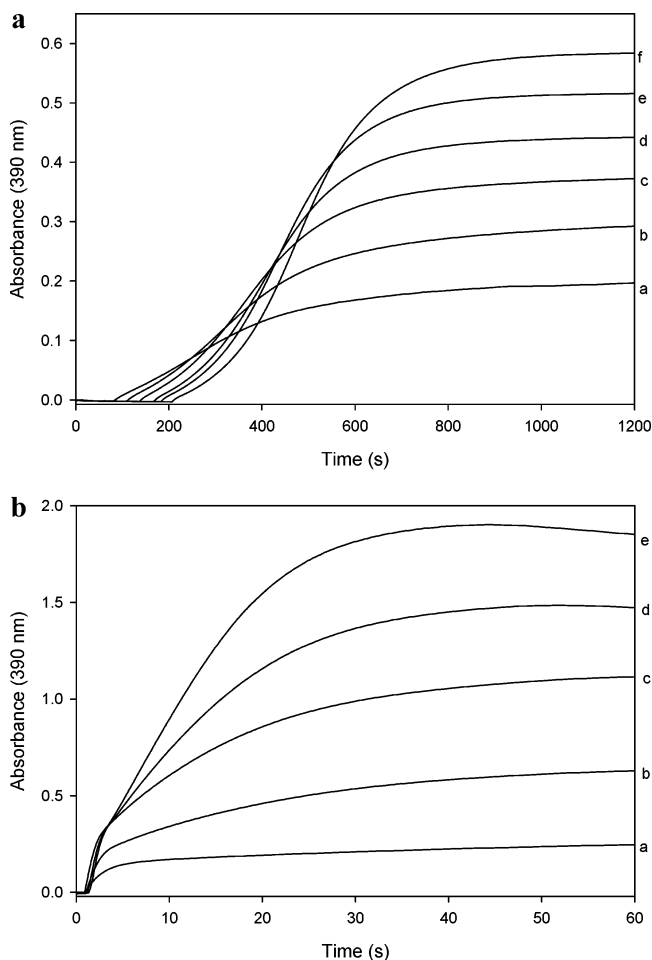


Figure 5. (A) In conditions with small oxidant to reductant ratios, for example, $5 > R > 4/3$, the induction period increases with TMTU concentrations since total consumption of TMTU is a prerequisite for formation of bromine. Fixed concentrations: $[\text{BrO}_3^-] = 1.0 \times 10^{-2} \text{ M}$, $[\text{HClO}_4] = 5.0 \times 10^{-1} \text{ M}$. Variable concentration: $[\text{TMTU}] =$ (a) $2.0 \times 10^{-3} \text{ M}$, (b) $2.6 \times 10^{-3} \text{ M}$, (c) $3.4 \times 10^{-3} \text{ M}$, (d) $3.9 \times 10^{-3} \text{ M}$, (e) $4.6 \times 10^{-3} \text{ M}$, or (f) $5.2 \times 10^{-3} \text{ M}$. (B) With an overwhelming excess of acidic bromate over TMTU, the induction period becomes invariant to changes in TMTU concentrations, but the rate and amount of bromine formed are now heavily dependent on initial TMTU concentrations. Fixed concentrations: $[\text{BrO}_3^-] = 2.0 \times 10^{-1} \text{ M}$, $[\text{HClO}_4] = 5.0 \times 10^{-1} \text{ M}$. Variable concentration: $[\text{TMTU}] =$ (a) $2.2 \times 10^{-3} \text{ M}$, (b) $5.6 \times 10^{-3} \text{ M}$, (c) $9.9 \times 10^{-3} \text{ M}$, (d) $1.3 \times 10^{-2} \text{ M}$, or (e) $1.7 \times 10^{-2} \text{ M}$.

the stoichiometric ratio of oxidant to reductant was greater than 8:5. The amount of bromine formed consistently decreased as this ratio was lowered until 4:3, when no bromine formation is observed, and the stoichiometry reverts to that shown in reaction R1.

Effect of TMTU. Under conditions in which the oxidant to reductant ratio was small, $1.33 < R < 1.6$, an increase in TMTU lengthened the induction period, increased the amount of bromine formed, and also increased the rate of formation of bromine at the end of the induction period (see Figure 5A). In high excess of bromate over TMTU ($R \gg 1.6$), however, the induction period becomes invariant to changes in initial TMTU concentrations but the rate and amount of bromine formed after the induction period increases with TMTU (see Figure 5B). Data in Figure 5 suggest that (i) the complete consumption of TMTU is a prerequisite for the formation of bromine, (ii) the Br_2 -TMTU reaction is much faster than the BrO_3^- -TMTU reaction, and (iii) bromine formation and rate of bromine formation is dependent upon a product derived from the BrO_3^- -TMTU

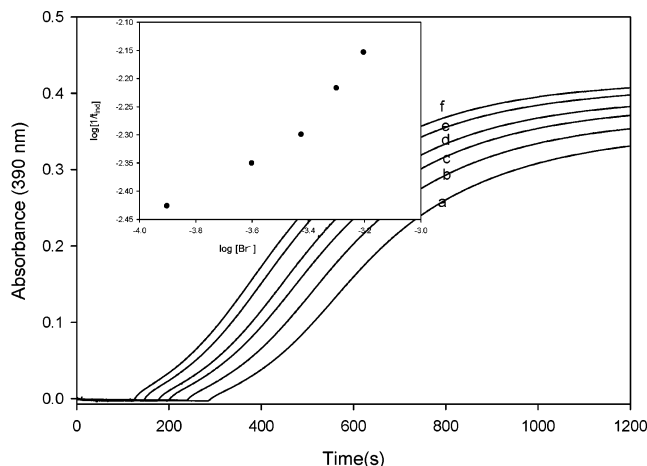


Figure 6. Effect of bromide, showing its autocatalytic nature (it is a product and yet accelerates the rate of reaction). Bromide decreases the induction period and increases both the amounts of bromine formed and the rate at which this bromine is formed. A log–log plot of bromide concentrations vs inverse of the induction period (shown in the inset) gives a concave shape, also indicative of autocatalysis. Fixed concentrations: $[\text{TMTU}]_0 = 3.0 \times 10^{-3}$ M, $[\text{BrO}_3^-]_0 = 5.0 \times 10^{-3}$ M, $[\text{HClO}_4]_0 = 6.25 \times 10^{-1}$ M. Variable concentration: $[\text{Br}^-] =$ (a) 0, (b) 1.25×10^{-4} M, (c) 2.5×10^{-4} M, (d) 3.75×10^{-4} M, (e) 5.0×10^{-4} M, or (f) 6.25×10^{-4} M.

reaction since both increase as TMTU is increased. This implicates Br^- , which is the reduction product of bromate and bromine.

Effect of Bromide. Bromide is strongly autocatalytic to the reaction (it is a product, and it also accelerates the reaction). Figure 6 shows that addition of bromide decreases the induction period and also increases the final amount of bromine produced for reactions with $R > 1.6$. With a ratio greater than 1.6, any additional bromide added to the reaction mixture (as in Figure 6), will contribute to the $\text{BrO}_3^- - \text{Br}^-$ reaction to produce additional bromine over that produced by the stoichiometry in reaction R2. The reduction in the induction period suggests that the $\text{BrO}_3^- - \text{Br}^-$ reaction should be a precursor reaction for the reactive species that control the oxidation of TMTU. A log–log plot of bromide concentrations versus the inverse of the induction period (Figure 6 inset) gives a plot with a constantly increasing slope, which indicates autocatalysis by bromide.

Detection at 216 nm. Figure 7 shows a series of absorbance traces monitored at 216 nm. Both Br_3^- and TMTU absorbed strongly at 216 nm, but at the beginning of the reaction, before their accumulation, an initial rate of reaction based on the consumption of TMTU could be experimentally estimated. First, a plot was made of the observed initial absorbances at 216 nm versus the initial concentrations of TMTU (see Figure 7 inset). An extrapolation of this plot to $[\text{TMTU}]_0 = 0.00$ M gave a reading that gave the background contribution from all other species in the reaction medium with no TMTU (top traces). This value was subtracted out of every absorbance data point to give the sole contribution of TMTU to the absorbance at 216 nm (bottom set of traces). The data show that the reaction is simple first-order with respect to TMTU.

Direct Br_2 –TMTU Reaction. Figure 8A shows, as expected from the data obtained on the effect of bromide on the reaction, that the direct oxidation of TMTU by bromine is much faster than the reaction between acidic bromate and TMTU. At slight excess of bromine over TMTU, the reaction is complete in less than 20 s. A plot of residual bromine absorbance after total

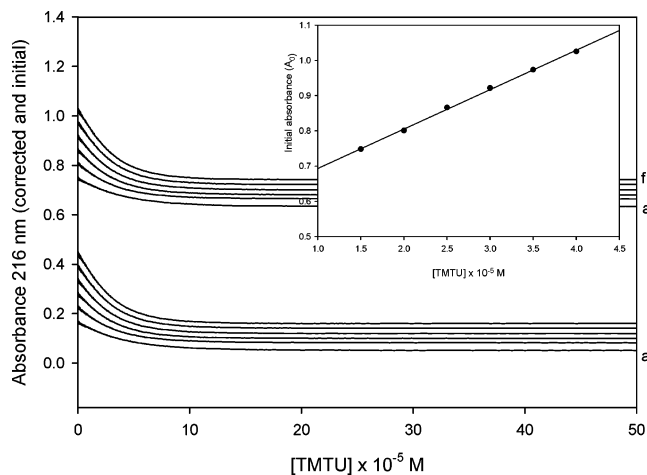


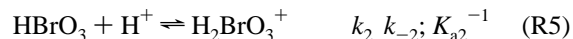
Figure 7. Absorbance traces at 216 nm (upper traces) and (inset) plot of initial absorbance readings vs TMTU concentrations. Extrapolation to zero concentrations gives the offset absorbance readings, representing the absorbance from other extraneous species. Taking this offset off gives the lower traces. Fixed concentrations: $[\text{BrO}_3^-] = 2.0 \times 10^{-3}$ M, $[\text{HClO}_4] = 5.0 \times 10^{-1}$ M. Variable concentration: $[\text{TMTU}] =$ (a) 1.5×10^{-5} M, (b) 2.0×10^{-5} M, (c) 2.5×10^{-5} M, (d) 3.0×10^{-5} M, (e) 3.5×10^{-5} M, or (f) 4.0×10^{-5} M.

consumption of TMTU gives the expected straight line (Figure 8B), with the intercept of this plot giving the exact amount of bromine needed to satiate stoichiometry R3, without excess bromine left. Figure 8B shows that, for a fixed concentration of 0.0005 M TMTU, the exact stoichiometric equivalent of bromine needed is 0.002 M, which serves to prove the 4:1 stoichiometry deduced in reaction R3. A plot of initial rate of reaction versus initial bromine concentrations shows simple first-order dependence with an intercept kinetically indistinguishable from 0 (Figure 8C). First-order dependence on TMTU was also observed (see Figure 8D and inset).

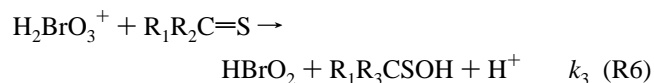
Mechanism. Bromate oxidizes only in highly acidic medium, which suggests that some degree of protonation of bromate is a prerequisite for its action as an oxidant:



Rabai et al.³⁷ have suggested that the key reactive intermediate is obtained after further protonation of HBrO_3 :



The rate-determining step for any bromate-derived oxidations of the thiuredo group becomes reaction R6:



Here $\text{R}_1 = \text{NMe}_2$, $\text{R}_2 = \text{NHMe}$, and $\text{R}_3 = (\text{MeN}=\text{})$. One can derive a general rate law based on reaction R6. If one assumes both BrO_3^- and HBrO_3 are inert species with respect to oxidation of TMTU, then one can derive the following relationships:

$$[\text{Br(V)}]_{\text{T}} = [\text{BrO}_3^-] + [\text{HBrO}_3] + [\text{H}_2\text{BrO}_3^+] \quad (1)$$

$$\text{rate} = -d[\text{R}_1\text{R}_2\text{C}=\text{S}]/dt = k_3[\text{R}_1\text{R}_2\text{C}=\text{S}][\text{H}_2\text{BrO}_3^+] \quad (2)$$

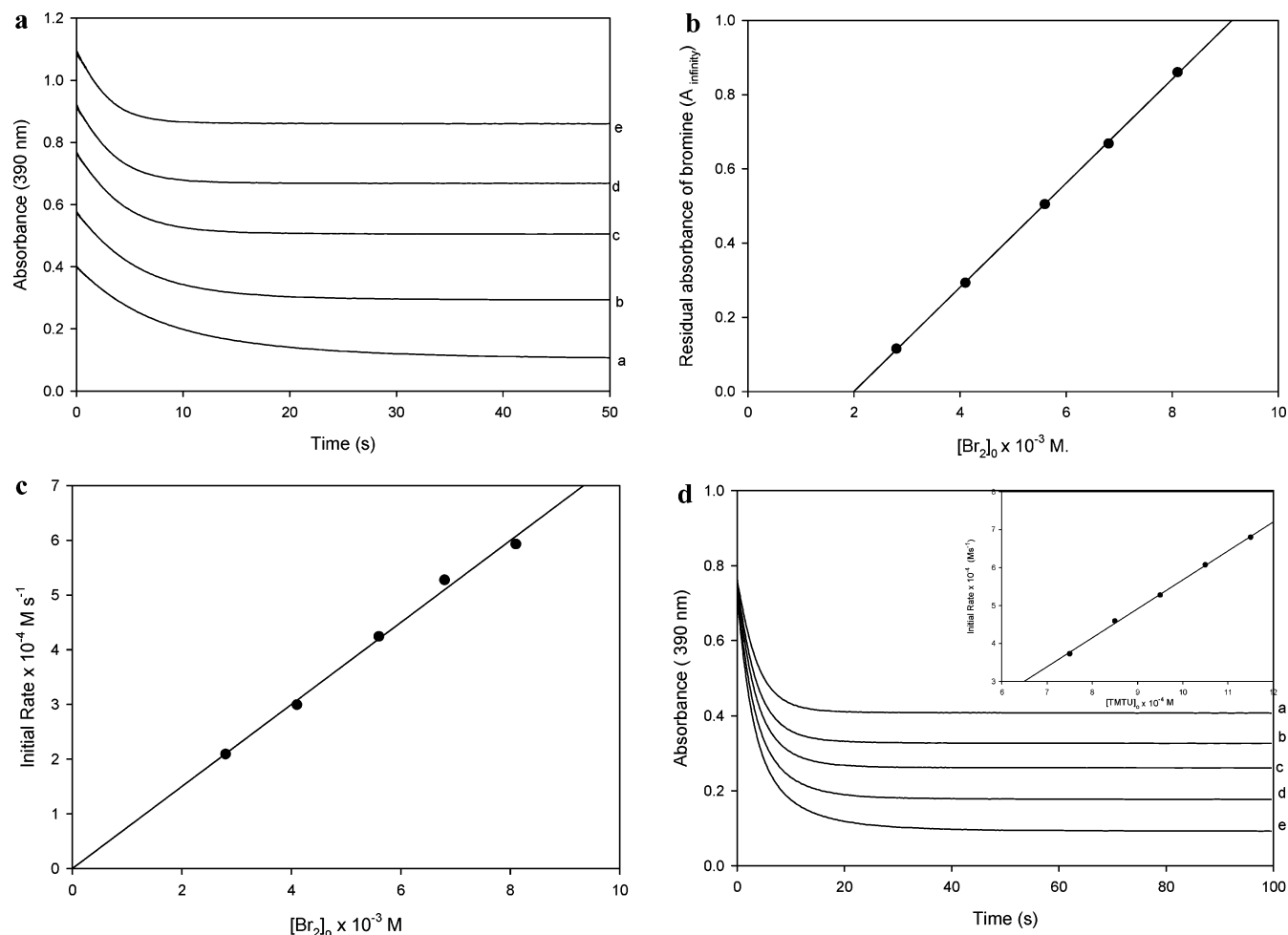


Figure 8. (A) Absorbance traces from the Br_2 -TMTU reaction in excess bromine conditions ($[\text{Br}_2]_0/[\text{TMTU}]_0 > 4$). The reaction is essentially complete in 10 s or less with a complete consumption of TMTU to TMU and sulfate. Fixed concentration: $[\text{TMTU}]_0 = 5.0 \times 10^{-4}$ M. Variable concentration: $[\text{Br}_2] =$ (a) 2.8×10^{-3} M, (b) 4.1×10^{-3} M, (c) 5.6×10^{-3} M, (d) 6.8×10^{-3} M, or (e) 8.1×10^{-3} M. (B) Residual bromine absorbance at infinity after consumption by TMTU (derived from data in panel A). This plot conclusively deduced the 4:1 stoichiometric ratio. Residual Br_2 absorbances are derived from excess Br_2 after all TMTU has been completely oxidized. The plot shows that, with 0.0005 M TMTU, exactly 0.002 M Br_2 is needed to completely consume this amount of TMTU (derived from the intercept of the Br_2 axis). (C) Initial rate plot from data in panel A. This plot shows that the reaction displays a strong first-order dependence on Br_2 concentrations, with an intercept kinetically indistinguishable from 0. (D) Effect of TMTU on the Br_2 -TMTU reaction. The reaction is also first-order in $[\text{TMTU}]_0$ (see inset). Fixed concentration: $[\text{Br}_2] = 5.90 \times 10^{-3}$ M. Variable concentration: $[\text{TMTU}] =$ (a) 7.5×10^{-4} M, (b) 8.5×10^{-4} M, (c) 9.5×10^{-4} M, (d) 10.5×10^{-4} M, or (e) 11.5×10^{-4} M.

$[\text{Br}(\text{V})]_{\text{T}}$ is the total bromate concentration in solution before it partitions out into bromic acid and protonated bromic acid. This will give the final rate of reaction:

$$\text{rate} = \frac{k_3[\text{R}_1\text{R}_2\text{C}=\text{S}][\text{Br}(\text{V})]_{\text{T}}[\text{H}^+]^2}{[\text{H}^+]^2 + K_{\text{a}2}[\text{H}^+] + K_{\text{a}1}K_{\text{a}2}} \quad (3)$$

In the limit of low acid concentrations, the rate of reaction reduces to

$$v = \frac{k_3[\text{R}_1\text{R}_2\text{C}=\text{S}][\text{Br}(\text{V})]_{\text{T}}[\text{H}^+]^2}{K_{\text{a}1}K_{\text{a}2}} \quad (4)$$

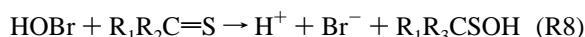
This agrees with our experimentally determined rate law. However, since we did not work at low acid concentrations, our experimental data put a limitation on the acceptable value for the product $K_{\text{a}1}K_{\text{a}2}$. The values of $K_{\text{a}1}$ and $K_{\text{a}2}$ themselves are not important for the establishment of the rate law, except that they should be of a magnitude that allows for the minimization of the other two terms in the denominator. There have been several studies on the value of $\text{p}K_{\text{a}1}$, all of which

differ and give values that range from -0.5 to 1.87 .^{38,39} By use of data in Figure 7, one can assume buffered acid concentrations to evaluate a lower limit to the value for k_3 :

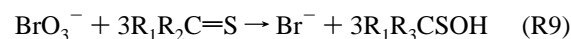
$$\text{rate} = k_{\text{app}}[\text{R}_1\text{R}_2\text{C}=\text{S}][\text{Br}(\text{V})]_{\text{T}} \quad (5)$$

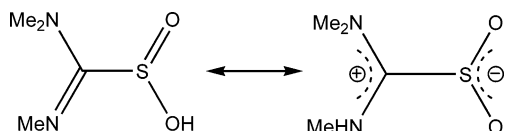
where $k_{\text{app}} = k_3[\text{H}^+]^2/K_{\text{a}1}K_{\text{a}2}$. This treatment gives a value of $k_{\text{app}} = 36.6 \pm 0.2 \text{ M}^{-1} \text{ s}^{-1}$ as a lower limit.

Initial Stages of the Reaction: Formation of Bromide. The initial stages involve the production of bromide, which acts as an autocatalyst in the reaction mechanism. From reaction R6, there is a successive reduction of bromate to bromide:



Addition of reactions R4–R8 gives the overall stoichiometry of the initial stages of the reaction as



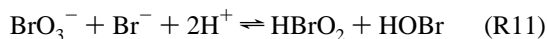
SCHEME 1: Zwitterionic Form of the Sulfinic Acid of TMTU

The six electrons needed in reaction R9 can be supplied by any of the oxidizable organosulfur species that have not yet been oxidatively saturated to sulfate and are not necessarily from the parent thiouredo compound.

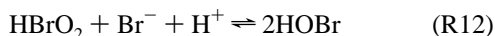
Autocatalytic Build-up of Bromide. The initial formation of bromide will initiate the standard oxybromine kinetics, which are dominated by reaction R11. Several previous studies have suggested that the rate-determining step in the oxidation of bromide by bromate is its reaction with protonated bromic acid (reaction R10).^{37,38}



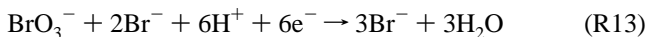
Addition of reactions R4 + R5 + R10 gives the well-known composite reaction R11:



Reaction R11 introduces the reactive oxybromine species that are responsible for the oxidizing abilities of acidic bromate. Although both bromous acid and hypobromous acid are oxidizing, the facile disproportionation of bromous acid to hypobromous acid (reaction R12) allows us to ignore oxidation by bromous acid and assume hypobromous acid as the major oxidizing species (reaction R8).



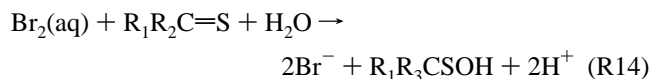
Addition of reactions R11 + R12 + 3R8 gives a final stoichiometry that involves cubic autocatalysis in bromide:



A simple simulation of reaction R13 will show an initially dramatic and sigmoidal increase in rate of bromide production with time, whose possible unchecked runaway production is contained only by depletion of bromate and substrate, thereby going through a maximum whose attainment is determined by the magnitude of the forward rate constant of reaction R11. The shape of the log–log plot of bromide concentration and rate, with its nonlinear ever-increasing response to bromide concentrations (see Figure 7, inset), proves that bromide is an autocatalyst in this reaction scheme.

Direct Oxidation of TMTU by Bromine. The oxidation of TMTU by aqueous bromine is a simple overall second-order

reaction with a bimolecular rate constant of $(1.50 \pm 0.04) \times 10^2 \text{ M}^{-1} \text{ s}^{-1}$. The rate-determining step is the initial oxidation of the thiouredo group to the unstable sulfinic acid:



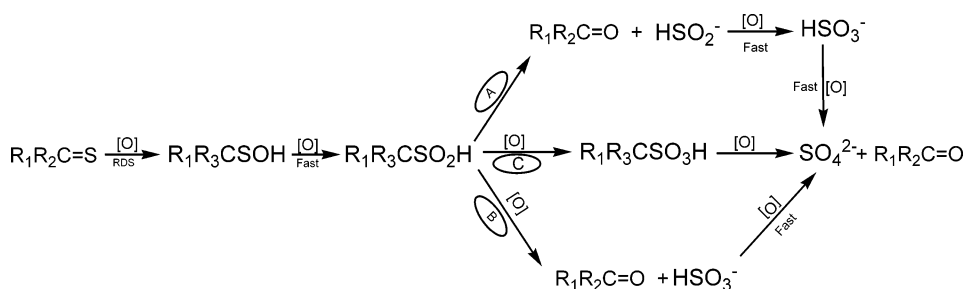
Further oxidations of the sulfinic acid and other metabolites should be facile. A previous study of the oxidation of unsubstituted thiourea by bromine had shown a much slower reaction, characterized by an initial fast phase in which over 2 equiv of bromine are consumed.⁴⁰ The slower last phase of the reaction (reaction time on the order of 10–20 min) delivered complex absorbance readings due to the participation of the Br_2/Br^- reaction to give Br_3^- , which has a higher absorptivity coefficient than bromine at 390 nm. This suggested the formation of stable oxidation intermediates such as the sulfinic and sulfonic acids, which are then slowly oxidized to sulfate. The oxidation of TMTU, on the other hand, went to completion in one phase, with formation of sulfate and its urea analogue as the final products.

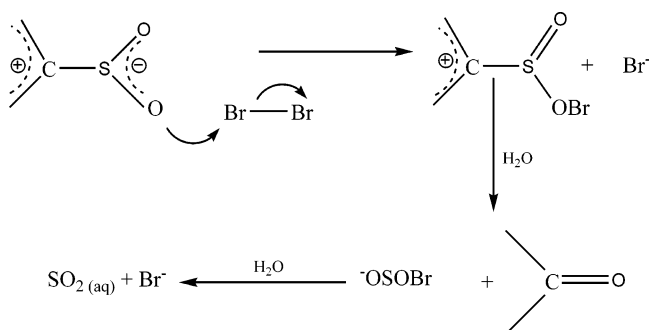
Oxidation Pathway of TMTU. The initial two-electron oxidation of TMTU gives the unstable sulfinic acid. In the absence of further oxidant, this sulfinic acid can either dimerize or disproportionate into more stable thiosulfonates. Further oxidation to the sulfonic acid should be rapid. The oxidation can be accomplished by any of the oxidizing species in solution, HBrO_2 , HOBr , or $\text{Br}_2(\text{aq})$, all of which are two-electron oxidants.



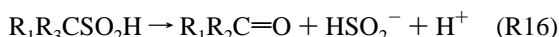
Structures and reactivities of thiouredo oxoacids have been studied extensively by Simoyi and co-workers.^{35,41} In acidic environments and in solid crystal form, the sulfinic and sulfonic acids exist predominantly and strictly in the zwitterionic form with the positive charge delocalized over the N–C–N three-center four-electron network (see Scheme 1). Such structures make the carbon center vulnerable to nucleophilic attack, especially from solvent molecules such as water, and that means most oxidations will have to occur from the sulfur center and not from the carbon center. The electrophilic oxidizing agents (e.g., Br_2 and HOBr in this case) will most likely attack the electron-rich sulfur oxoacid group.

Three possible routes exist for further oxidation of the sulfinic acid (see Scheme 2, pathways A, B, and C). Previous studies on the oxidation pathways of thiourea compounds have concluded that if the sulfonic acid is formed, it should be very stable and resistant to further oxidation except in highly basic environments. The sulfinic acids, on the other hand, possess a very long C–S bond that is easily cleaved heterolytically, to produce a very reactive and highly reducing sulfur leaving

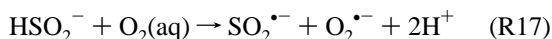
SCHEME 2: Oxidation Route of TMTU

SCHEME 3: Direct Oxidation of TMTU Sulfinic Acid through Pathway B

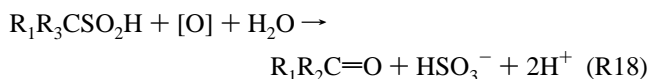
group, the sulfoxylate anion-radical (reaction R16 and pathway A).^{42–44}



Proof of the dominance of reaction R16 was derived from the observation that neutral to basic solutions of thiouredo sulfinic acids produced dithionite upon standing in aerobic conditions.⁴³ Precursor for dithionite is $\text{SO}_2^{\bullet-}$, which is derived from the diffusion-controlled autoxidation of HSO_2^- :

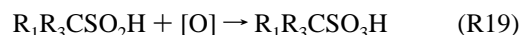


Strictly anaerobic conditions did not afford dithionite. The superoxide radicals produced and the subsequent cascade of reactive oxygen species could be observed by their characteristic electron paramagnetic resonance (EPR) spectra in combination with a suitable trap. Reaction R16, however, is strongly favored in basic environments but would be insignificant in the strongly acidic environments relevant to bromate oxidations. Another oxidation route for the sulfinic acid would involve the cleavage of the C–S bond, coupled with the oxidation of the sulfur leaving group to S(IV), bisulfite (pathway B).

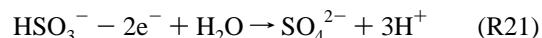
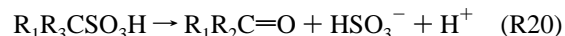


Scheme 3 shows how a typical electrophilic attack on the sulfinic acid can lead to pathway B.

Further oxidation of bisulfite should be facile and fast.⁴⁵ Pathway C would involve the further oxidation of the sulfinic acid to the sulfonic acid:



The sulfonic acid would then be further oxidized through pathway A or B as well.



Pathway through the sulfonic acid is attained only by controlled oxidation of the sulfinic acid, by use of stoichiometric amounts of a weak oxidant such as peracetic acid, and at very low temperatures to slow down the rate of reaction. The sulfonic acid, once formed, is very stable and immune to further oxidation. It can only be further oxidized through an initial hydrolysis (reaction R20). The sulfonic acid is very stable in acidic conditions due to formation of the stable zwitterion. Stoichiometric formation of sulfate would be achieved only after prolonged standing and aging of the reaction solutions. The fact that stoichiometric equivalence was achieved in less than 10 s for bromine oxidations of TMTU (for example) precludes pathway C as a major route of oxidation. The highly acidic environments used in these bromate oxidations also preclude pathway A as being a major oxidation pathway. The zwitterion is strongly stabilized by the low-pH environments used in these oxidations. Only in highly basic environments would pathway A be dominant.

Overall Mechanism and Computer Simulations. The proposed mechanism is simplified greatly by the rapid oxidation of TMTU by aqueous bromine. So fast is this oxidation that it is about an order of magnitude greater than the comparable oxidation of TMTU by bromate, which is controlled, initially, by reaction R11. If these two reactions were of comparable magnitude, then oligooscillatory production of bromine would be observed in which the concentration of bromine would display at least two peaks.⁴⁶ Other thiouredo group oxidations show complex kinetics due to the nonuniform oxidation of the sulfur center to sulfate.⁴⁶ The nonlinearities arise mostly from the formation of stable sulfinic and sulfonic acid intermediates, which are difficult to oxidize further. TMTU's oxidation by acidic bromate displays

TABLE 2: Trimethylthiourea (TMTU)–Bromate/Bromine Reaction Scheme

no.	reaction	k_f, k_r
M1	$\text{BrO}_3^- + \text{H}^+ \rightleftharpoons \text{HBrO}_3$	$1.0 \times 10^9; 3.16 \times 10^8$
M2	$\text{HBrO}_3 + \text{H}^+ \rightleftharpoons \text{H}_2\text{BrO}_3^+$	$1.0 \times 10^7; 5.0 \times 10^9$
M3	$\text{H}_2\text{BrO}_3^+ + \text{R}_1\text{R}_2\text{CS} \rightarrow \text{R}_1\text{R}_3\text{CSOH} + \text{HBrO}_2$	36
M4	$\text{HBrO}_2 + \text{R}_1\text{R}_2\text{CS} \rightarrow \text{R}_1\text{R}_3\text{CSOH} + \text{HOBr}$	45
M5	$\text{HOBr} + \text{R}_1\text{R}_2\text{CS} \rightarrow \text{R}_1\text{R}_3\text{CSOH} + \text{H}^+ + \text{Br}^-$	5.0×10^2
M6	$\text{HOBr} + \text{Br}^- + \text{H}^+ \rightleftharpoons \text{Br}_2 + \text{H}_2\text{O}$	$8.9 \times 10^8; 110$
M7	$\text{BrO}_3^- + \text{Br}^- + 2\text{H}^+ \rightleftharpoons \text{HBrO}_2 + \text{HOBr}$	$2.1; 1.0 \times 10^4$
M8	$\text{HBrO}_2 + \text{Br}^- + \text{H}^+ \rightleftharpoons 2\text{HOBr}$	$2.0 \times 10^9; 5.0 \times 10^{-5}$
M9	$\text{HOBr} + \text{R}_1\text{R}_3\text{CSOH} \rightarrow \text{R}_1\text{R}_3\text{CSO}_2\text{H} + \text{Br}^- + \text{H}^+$	3.0×10^4
M10	$\text{HOBr} + \text{R}_1\text{R}_3\text{CSO}_2\text{H} \rightarrow \text{HSO}_3^- + \text{R}_1\text{R}_2\text{C}=\text{O} + \text{H}^+$	5.0×10^3
M11	$\text{HOBr} + \text{HSO}_3^- + \text{H}^+ \rightarrow \text{SO}_4^{2-} + \text{Br}^- + 2\text{H}^+$	1.0×10^{10}
M12	$\text{Br}_2 + \text{R}_1\text{R}_2\text{C}=\text{S} \rightarrow \text{R}_1\text{R}_2\text{CSOH} + 2\text{H}^+ + 2\text{Br}^-$	150
M13	$\text{Br}_2 + \text{R}_1\text{R}_3\text{CSOH} \rightarrow \text{R}_1\text{R}_3\text{CSO}_2\text{H} + 2\text{H}^+ + 2\text{Br}^-$	1.0×10^3
M14	$\text{Br}_2 + \text{R}_1\text{R}_3\text{CSO}_2\text{H} \rightarrow \text{R}_1\text{R}_3\text{CSO}_3\text{H} + 2\text{H}^+ + 2\text{Br}^-$	5.0×10^{-3}
M15	$\text{Br}_2 + \text{R}_1\text{R}_3\text{CSO}_3\text{H} + 2\text{H}_2\text{O} \rightarrow \text{R}_1\text{R}_2\text{C}=\text{O} + \text{SO}_4^{2-} + 2\text{Br}^- + 5\text{H}^+$	1.0×10^{-3}
M16	$\text{R}_1\text{R}_3\text{CSO}_2\text{H} + \text{H}_2\text{O} \rightarrow \text{HSO}_2^- + \text{R}_1\text{R}_2\text{C}=\text{O} + \text{H}^+$	10
M17	$\text{R}_1\text{R}_3\text{CSO}_3\text{H} + \text{H}_2\text{O} \rightarrow \text{HSO}_3^- + \text{R}_1\text{R}_2\text{C}=\text{O} + \text{H}^+$	5.0×10^{-1}
M18	$\text{HSO}_2^- + \text{Br}_2 + \text{H}_2\text{O} \rightarrow \text{HSO}_3^- + 2\text{H}^+ + 2\text{Br}^-$	5.0×10^7
M19	$\text{HSO}_3^- + \text{Br}_2 + \text{H}_2\text{O} \rightarrow \text{SO}_4^{2-} + 3\text{H}^+ + 2\text{Br}^-$	1.0×10^8
M20	$\text{Br}_2 + \text{R}_1\text{R}_3\text{CSO}_2\text{H} + 2\text{H}_2\text{O} \rightarrow \text{HSO}_3^- + \text{R}_1\text{R}_2\text{C}=\text{O} + 2\text{Br}^- + 4\text{H}^+$	200

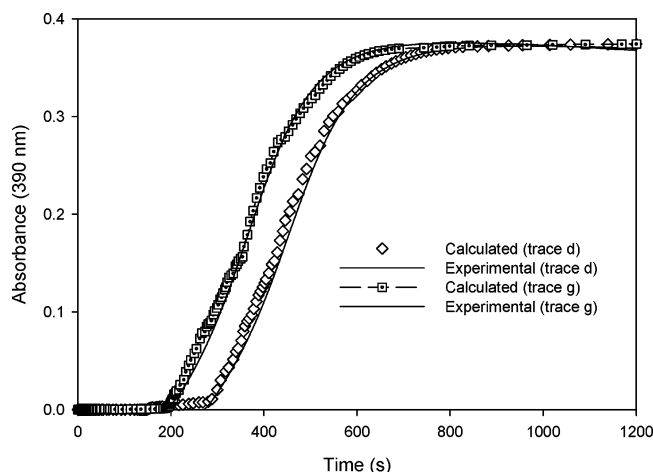


Figure 9. Comparison of experimental and calculated absorbance traces for the bromate variation shown in Figure 4 (traces d and g). Symbols represent the simulated results.

no such added nonlinearities (apart from those generated by the oxybromine chemistry) because after the initial two-electron oxidation of the sulfur center to form the sulfenic acid, the rest of the stepwise oxidations are facile and rapid. Hence our postulated mechanism leans heavily on the oxybromine kinetics, and all generated nonlinearities are those that can be expected from oxybromine chemistry.¹⁹ A 20-reaction mechanism is proposed and shown in Table 2. Most of the kinetics parameters are known (oxybromine) and derived from literature values.^{18,19,38,47,48} Reaction M1 (R4), was assumed to be a fast protolytic reaction, and the ratio of k_f and k_r was set by the literature value of the pK_a of bromic acid.^{38,39} Reaction M3 could be handled as a termolecular process of TMTU, bromic acid, and H^+ . k_3 would then be adjusted to account for the acid concentration, which we assumed to be constant and buffered in this model. The bromine–TMTU rate constants were derived from this study. Without bromide added initially to the reaction mixtures, the simulations fit relied heavily on the rate of the initial oxidation of TMTU (reaction R6, forward rate constant k_3) because this determined the initial rate of formation of the autocatalyst, bromide. However, in conditions in which bromide was initially added to the reaction mixture, the value of k_3 became irrelevant as the reaction's overall dynamical behavior (induction period and rate of formation of bromine at the end of the induction period) was now determined solely by reaction M7 (R11). An initial estimation of k_3 was made from the data shown in Figure 7. The low-pH conditions used in our study made oxidations by HOBr relatively unimportant compared to oxidations through molecular bromine. Hence simulations were insensitive to kinetics parameters used for reactions M9–M11. After establishment of k_{M12} (forward rate constant for M12), the other rate constants could be set at any value as long as they were not rate-determining.

Figure 9 shows a reasonably good fit to the data in Figure 4 on the effect of progressively increasing bromate concentration.

Conclusion

The oxidations of substituted thioureas, despite their structural similarities, display a wide variety of dynamical behavior. The same applies in the physiological environment where similar compounds, with the same thioureido group in common, also display very varied physiological effects. The dynamics observed in the forerunners of this paper (S-oxygenation, parts 1 and 2)¹ display much more complex kinetics due to the more

stable metabolites formed during the oxidation of phenylthiourea^{1a} (S-Oxy 1) and due to the autocatalytic oxidation of TMTU^{1b} by chlorine dioxide (S-Oxy 2). None of these complexities feature in this oxidation and hence the kinetics and dynamics are simpler. Our attempts at synthesizing the sulfinic and sulfonic acids of TMTU also failed due to the reactivities of these metabolites.

Acknowledgment. This work was supported by Research Grant CHE 0614924 from the National Science Foundation.

References and Notes

- (1) (a) Part 1: Chigwada, T. R.; Chikwana, E.; Simoyi, R. H. *J. Phys. Chem. A* **2005**, *109*, 1081–1093. (b) Part 2: Chigwada, T. R.; Simoyi, R. H. *J. Phys. Chem. A* **2005**, *109*, 1094–1104.
- (2) Chinake, C. R.; Simoyi, R. H. *J. Phys. Chem.* **1993**, *97*, 11569–11570.
- (3) Rabai, G.; Orban, M.; Epstein, I. R. *Acc. Chem. Res.* **1990**, *23*, 258–263.
- (4) Orban, M.; De Kepper, P.; Epstein, I. R. *J. Phys. Chem.* **1982**, *86*, 431–433.
- (5) Rabai, G.; Orban, M.; Epstein, I. R. *J. Phys. Chem.* **1992**, *96*, 5414–5419.
- (6) Rabai, G.; Epstein, I. R. *J. Am. Chem. Soc.* **1992**, *114*, 1529–1530.
- (7) Simoyi, R. H. *J. Phys. Chem.* **1986**, *90*, 2802–2804.
- (8) Simoyi, R. H.; Wolf, A.; Swinney, H. L. *Phys. Rev. Lett.* **1982**, *49*, 245–248.
- (9) Doona, C. J.; Blittersdorf, R.; Schneider, F. W. *J. Phys. Chem.* **1993**, *97*, 7258–7263.
- (10) Hauser, M. J. B.; Chinake, C. R.; Simoyi, R. H. *S. Afr. J. Chem.* **1995**, *48*, 135–141.
- (11) Epstein, I. R.; Kustin, K.; Simoyi, R. H. *J. Phys. Chem.* **1992**, *96*, 6326–6331.
- (12) Scott, A. M.; Powell, G. M.; Upshall, D. G.; Curtis, C. G. *Environ. Health Perspect.* **1990**, *85*, 43–50.
- (13) Rabai, G.; Beck, M. T. *J. Chem. Soc., Dalton Trans.* **1985**, 1669–1672.
- (14) Epstein, I. R.; Kustin, K.; Simoyi, R. H. *J. Phys. Chem.* **1992**, *96*, 5852–5856.
- (15) Jonnalagadda, S. B.; Chinake, C. R.; Simoyi, R. H. *J. Phys. Chem.* **1996**, *100*, 13521–13530.
- (16) Doona, C. J.; Doumbouya, S. I. *J. Phys. Chem.* **1994**, *98*, 513–517.
- (17) Martincigh, B. S.; Hauser, M. J. B.; Simoyi, R. H. *Phys. Rev. E* **1995**, *52*, 6146–6153.
- (18) Noyes, R. M.; Field, R. J.; Thompson, R. C. *J. Am. Chem. Soc.* **1971**, *93*, 7315–7316.
- (19) Noyes, R. M. *J. Am. Chem. Soc.* **1980**, *102*, 4644–4649.
- (20) *Natl. Toxicol. Program, Tech. Rep. Ser.* **1992**, *388*, 1–256.
- (21) Hollinger, M. A.; Giri, S. N.; Alley, M.; Budd, E. R.; Hwang, F. *Proc. West. Pharmacol. Soc.* **1975**, *18*, 351–353.
- (22) Hollinger, M. A.; Giri, S. N.; Alley, M.; Budd, E. R.; Hwang, F. *Drug Metab. Dispos.* **1974**, *2*, 521–525.
- (23) Hollinger, M. A.; Giri, S. N.; Hwang, F.; Budd, E. R. *Res. Commun. Chem. Pathol. Pharmacol.* **1974**, *8*, 319–326.
- (24) Kim, S. G.; Kim, H. J.; Yang, C. H. *Chem.-Biol. Interact.* **1999**, *117*, 117–134.
- (25) Poulsen, L. L.; Hyslop, R. M.; Ziegler, D. M. *Arch. Biochem. Biophys.* **1979**, *198*, 78–88.
- (26) Scott, A. M.; Powell, G. M.; Upshall, D. G.; Curtis, C. G. *Environ. Health Perspect.* **1990**, *85*, 43–50.
- (27) Ziegler-Skylakakis, K.; Nill, S.; Pan, J. F.; Andrae, U. *Environ. Mol. Mutagen.* **1998**, *31*, 362–373.
- (28) Onderwater, R. C.; Commandeur, J. N.; Vermeulen, N. P. *Toxicology* **2004**, *197*, 81–91.
- (29) Uckun, F. M.; Pendergrass, S.; Maher, D.; Zhu, D.; Tuel-Ahlgren, L.; Mao, C.; Venkatachalam, T. K. *Bioorg. Med. Chem. Lett.* **1999**, *9*, 3411–3416.
- (30) Toth, K. M.; Harlan, J. M.; Beehler, C. J.; Berger, E. M.; Parker, N. B.; Linas, S. L.; Repine, J. E. *Free Radical Biol. Med.* **1989**, *6*, 457–466.
- (31) Lam, S.; Tso, M. O.; Gurne, D. H. *Arch. Ophthalmol.* **1990**, *108*, 1751–1757.
- (32) Beehler, C. J.; Simchuk, M. L.; McCord, J. M.; Repine, J. E. *J. Lab. Clin. Med.* **1992**, *119*, 508–513.
- (33) Fox, R. B. *J. Clin. Invest.* **1984**, *74*, 1456–1464.
- (34) Makarov, S. V.; Mundoma, C.; Penn, J. H.; Svarovsky, S. A.; Simoyi, R. H. *J. Phys. Chem. A* **1998**, *102*, 6786–6792.

- (35) Makarov, S. V.; Mundoma, C.; Penn, J. H.; Petersen, J. L.; Svarovsky, S. A.; Simoyi, R. H. *Inorg. Chim. Acta* **1999**, *286*, 149–154.
- (36) Otoikhian, A.; Simoyi, R. H.; Petersen, J. L. *Chem. Res. Toxicol.* **2005**, *18*, 1167–1177.
- (37) Rabai, Gy.; Bazsa, Gy.; Beck, T. M. *Int. J. Chem. Kinet.* **1981**, *13*, 1277–1288.
- (38) Cortes, C. E. S.; Faria, R. B. *J. Braz. Chem. Soc.* **2001**, *12*, 775–779.
- (39) Kamble, D. L.; Nandibewoor, S. T. *Int. J. Chem. Kinet.* **1996**, *28*, 673–679.
- (40) Simoyi, R. H.; Epstein, I. R. *J. Phys. Chem.* **1987**, *91*, 5124–5128.
- (41) Makarov, S. V.; Mundoma, C.; Penn, J. H.; Svarovsky, S. A.; Simoyi, R. H. *J. Phys. Chem. A* **1998**, *102*, 6786–6792.
- (42) Makarov, S. V.; Mundoma, C.; Svarovsky, S. A.; Shi, X.; Gannett, P. M.; Simoyi, R. H. *Arch. Biochem. Biophys.* **1999**, *367*, 289–296.
- (43) Svarovsky, S. A.; Simoyi, R. H.; Makarov, S. V. *J. Chem. Soc., Dalton Trans.* **2000**, 511–514.
- (44) Svarovsky, S. A.; Simoyi, R. H.; Makarov, S. V. *J. Phys. Chem. B* **2001**, *105*, 12634–12643.
- (45) Hartz, K. E. H.; Nicoson, J. S.; Wang, L.; Margerum, D. W. *Abstr. Pap.—Am. Chem. Soc.* **2002**, *224*, U747.
- (46) Olagunju, O.; Siegel, P. A.; Olojo, R.; Simoyi, R. H. *J. Phys. Chem. A* **2006**, *110*, 2396–2410.
- (47) Jonnalagadda, S. B.; Chinake, C.; Simoyi, R. H. *J. Chem. Soc., Faraday Trans.* **1995**, *91*, 1635–1640.
- (48) Szalai, I.; Osolonovitch, J.; Forsterling, H. D. *J. Phys. Chem. A* **2000**, *104*, 1495–1498.